

Supporting Information

Fine-tuning the Chemical Passivation over photovoltaic perovskites by

Varying the Symmetry of Bidentate Acceptor in D-A Molecules

Minghuang Guo,^{1†} Jianbin Xu,^{2,3†} Jinting Li,¹ Jianting Huang,¹ Jingwei Zhu,¹ Yafeng Li,^{1*} Peng Gao,^{2,3*} Junming Li,¹ Mingdeng Wei^{1*}

¹ Fujian Key Laboratory of Electrochemical Energy Storage Materials, Fuzhou University, Xueyuan Road NO.2, Minhou, Fuzhou, Fujian 350116, China

² Fujian Science & Technology Innovation Laboratory for Optoelectronic Information of China, Fuzhou, Fujian 350108, China

³ Laboratory of Advance Functional Materials, Xiamen Institute of Rare Earth Materials, Haixi Institute, Chinese Academy of Science, Xiamen 361005, China

[†] *these authors contributed equally to this work*

** Corresponding authors*

Email addresses: liyf@fzu.edu.cn; peng.gao@fjirsm.ac.cn; wei-mingdeng@fzu.edu.cn

Experimental section

4.1 Materials

All the commercial materials were used as received without further purification. FAI, MAI, FK209, Li-TFSI, CsI, PbBr₂, tBP, and Spiro-OMeTAD were purchased from Xi'an Polymer Light Technology Corp. PbI₂ (99.9985%) was purchased from Alfa Aesar. Chlorobenzene, titanium diisopropoxide bis(acetylacetonate), 1-Butanol, N,N-dimethylformamide (DMF), and dimethyl sulfoxide (DMSO) were purchased from Sigma-Aldrich. Glass substrates with a transparent F-SnO₂ (FTO) (8 Ω/square) layer were purchased from Suzhou ShangYang Solar Technology Co., Ltd.

4.2 Synthesis of bidentate molecules

***N,N*-bis(4-methoxyphenyl)aniline (1)**. p-methoxy iodobenzene (4.1 g, 17.52 mmol), 1,10-Phenanthroline (0.25 g, 1.40 mmol), CuI (0.27 g, 1.40 mmol), t-BuOK (6.3g, 56.25 mmol) were added into a 100 ml flask. Then, toluene (23 ml) was charged to the flask, followed by aniline (0.63 ml, 6.88 mmol). The mixed reaction solution was refluxed overnight under N₂. After cooling to room temperature, the reaction solution was filtered to remove the precipitated base and extracted with dichloromethane and water. The crude product was separated by column chromatography with hexane. The isolated yield of the product was 76 %. ¹H-NMR (400 MHz, CDCl₃): δ 7.17 (t, J = 7.9 Hz, 2H), 7.05 (d, J = 8.9 Hz, 4H), 6.94 (d, J = 7.8 Hz, 2H), 6.88 (t, J = 7.3 Hz, 1H), 6.83 (d, J = 8.9 Hz, 4H), 3.80 (s, 6H).

4-(bis(4-methoxyphenyl)amino)benzaldehyde (2). Under an N₂ atmosphere, N,N-bis(4-methoxyphenyl)aniline (1) (1.7 g, 5.57 mmol) was dissolved in dry DMF (20 mL). After the flask was cooled to 0 °C, POCl₃ (0.78 mL, 8.35 mmol) was added dropwise into the mixture via a syringe. The reaction mixture was heated at 90 °C for 3 h and cooled to room temperature. The reaction was quenched with H₂O, extracted with ethyl acetate, and dried over MgSO₄. The residue was subjected to column chromatography on silica gel (hexane/ethyl acetate = 5/1, v/v), affording compound 2 as a yellow liquid (1.60 g, 86.49 %). ¹H-NMR (400 MHz, CDCl₃): δ 9.75 (s, 1H), 7.62 (d, J = 12.0 Hz, 2H), 7.13 (d, J = 8.0 Hz, 4H), 6.89 (t, J = 8.0 Hz, 4H), 6.84 (d, J = 12.0 Hz, 2H), 3.81 (s, 6H).

2-(4-(Bis(4-methoxyphenyl)amino)benzylidene)malononitrile (TA-MN). 4-[bis(4-methoxyphenyl)amino]benzaldehyde (2) (0.78 g, 2.28 mmol) was dissolved in dry N,N-dimethylformamide (15 mL) and added into 100 ml flask with NaOAc (0.28 g, 3.43 mmol). Then, malonodinitrile (0.15 ml, 2.28 mmol) was added to the mixture solution and reacted at room temperature. After 3 h, the reaction mixture was extracted with ethyl acetate and water, and dried over Mg₂SO₄. The residue was purified by column chromatography with the eluent of ethyl acetate/hexane (1:5, v/v). The product was recrystallized from hexane, and the orange crystals were afforded (0.46 g, 53%). ¹H-NMR (500 MHz, CDCl₃): δ 7.69 (d, J = 9.0 Hz, 2H), 7.47 (s, 1H), 7.14 (d, J = 9.0 Hz, 4H), 6.92 (d, J = 2.2 Hz, 4H), 6.80 (d, J = 9.1 Hz, 2H), 3.82 (s, 6H). ¹³C-NMR (500 MHz, CDCl₃): δ 157.95, 157.79, 154.19, 137.77, 133.19, 128.17, 121.72, 116.61, 115.55, 115.25, 114.43, 74.02, 55.55.

(Z)-3-(4-(bis(4-methoxyphenyl)amino)phenyl)-2-cyanoacrylic acid (TA-CA). In a

100 ml flask, 4-[bis(4-methoxyphenyl)amino]benzaldehyde (2) (1.03 g, 3.02 mmol), cyanoacetic acid (0.51 g, 6.04 mmol) and NaOAc (1.24 g, 9.06 mmol) were dissolved in dry DMF (20 mL) under a nitrogen atmosphere. Thereafter, the mixture was stirred at 60 °C for 6 h, and cooled to room temperature, then extracted with ethyl acetate and water. The crude product was eluted by column chromatography in a mixture of ethyl acetate: hexane=4:1, and 1% MeOH and 1% acetic acid were also added into the eluent. The product was recrystallized with hexane to gain pink crystals (0.45g 37.5%). ¹H-NMR (500 MHz, CDCl₃): δ 8.10 (s, 1H), 7.84 (d, J = 9.0 Hz, 2H), 7.14 (d, J = 8.9 Hz, 4H), 6.91 (d, J = 8.9 Hz, 4H), 6.83 (d, J = 9.1 Hz, 2H), 3.82 (s, 6H). ¹³C-NMR (500 MHz, CDCl₃): δ 169.36, 157.72, 155.47, 153.80, 138.11, 133.97, 128.12, 121.79, 116.82, 116.63, 115.18, 94.56, 55.55.

4.3 Device fabrication

FTO glass was etched by Zn power and diluted HCl solution, then cleaned with a detergent solution, deionized water, ethyl alcohol, acetone, and isopropyl alcohol in ultrasonic apparatus for 30 min. The compact TiO₂ layer was deposited onto FTO glass by spin-coating at a speed of 2000 rpm for 30 s, with the solution of 0.15 M of titanium diisopropoxide bis(acetylacetonate) in 1-Butanol, and then heated at 500 °C for 30 min. Next, a mesoporous layer was spin-coated by TiO₂ paste (Dyesol, 30NRD) at a speed of 2000 rpm for 30 s and heated at 550 °C for 30 min. The perovskite films were deposited using a single-step deposition method from the precursor solution, which was prepared in a nitrogen atmosphere, and the perovskite precursor solution was composed of 1.36 M FAI, 0.16 M MAI, 0.08 M CsI, 1.52 M PbI₂ and 0.16 M PbBr₂ in anhydrous DMF/DMSO = 4:1 (v:v). Then, the perovskite solutions were spin-coated on the substrates at 1000 rpm for 10 s and 4000 rpm for 20 s, respectively. During the second step, 100 uL of chlorobenzene with or without bidentate molecules were dropped 5 s before the end, followed by a heat treatment at 100 °C for 60 min. Finally, the Spiro-OMeTAD chlorobenzene solution (60 mM) mixed with 28.8 μL of 4-tert-butylpyridine, 17.5 μL of lithium bis(trifluoromethyl-sulfonyl)imide (520 mg·mL⁻¹ in acetonitrile) and 29.0 μL of cobalt bis(trifluoromethylsulfonyl)imide (300 mg·mL⁻¹ in acetonitrile) was spin-coated (4000 rpm for 30 s) on the top as a hole transporting layer. In the end, the gold layer was thermally evaporated to form a back electrode.

FAMA-based perovskite film fabrication: 1.0 M FAI, 0.22 M MABr, 1.1 M PbI₂ and 0.22 M PbBr₂ were dissolved in the DMF/DMSO = 4:1 (v:v) solution, and stirring 2 h under room temperature. The following fabrication is the same as the CsFAMA-based perovskite.

MAPbI₃ perovskite film fabrication: 1.3 M PbI₂ and 1.3 M MAI were dissolved in the DMF/DMSO (4:1 (v:v)) solution, and stirring 2 h under room temperature. Then, the perovskite solutions were spin-coated on the substrates at 1000 rpm for 10 s and 4000 rpm for 30 s, respectively. During the second step, 100 uL of chlorobenzene with or without bidentate molecules were dropped 8 s after start, followed by a heat treatment at 100 °C for 15 min.

4.4 Characterization

The crystallographic information for the perovskite films was measured by Rigaku Ultima IV with a conventional copper target X-ray tube set to 40 kV and 30 mA (Kα

radiation, 1.5418 Å). The morphology and structure of the samples were characterized by the field emission scanning electron microscope (FESEM, Hitachi S4800). The absorption spectra of the perovskite films and PbI_2 in DMF solution were measured by UV-vis spectrometry using a UV-2450 (Shimadzu). Atomic force microscopy (AFM) measurements were obtained using a SPA-5500 AFM (Bruker), and the scanning range of the AFM images was $5\ \mu\text{m} \times 5\ \mu\text{m}$. The steady-state photoluminescence (PL) and time-resolved photoluminescence spectroscopy (TRPL) of perovskite films/glass and HTM/perovskite/glass were performed using Edinburgh FLS 980 instrument with the excitation at 450 nm. PL intensity mapping was obtained by a confocal Raman spectrometer (LabRAM HR Evolution, Horiba scientific). Electroluminescence (EL) of the PSCs were performed using confocal Raman spectrometer (LabRAM HR Evolution, Horiba scientific) at 1.5 V bias under dark. IR spectra were measured on Thermo Fisher, Nicolet Is 50. XPS measurements were performed on a Thermo ESCALAB 250Xi instrument with a monochromatized Al $K\alpha$ X-ray source in a vacuum. The photovoltaic performance of PSCs was recorded using a source meter (Keithley 2400), a PEC-L11 1.5 solar simulator with a 1000 W Xe lamp, and an AM 1.5 filter (Peccell) was applied as the light source ($100\ \text{mW} \cdot \text{cm}^{-2}$). The J - V curves for the devices were measured from both forward (-0.2 to 1.2 V), or reverse (1.2 to -0.2 V) scan directions, and the scan rate was $20\ \text{mV} \cdot \text{s}^{-1}$. The devices were masked using a metal mask with a window of $0.12\ \text{cm}^2$ to define the active area. The Incident photon-to-electron conversion efficiency (IPCE) spectrum was recorded using an instrument of PEC-S20 (Peccell). Electrochemical Impedance Spectroscopy (EIS) spectrum was measured by an electrochemical workstation (IM6, Zahner) and fitting use software called Z-view.

4.5 DFT calculation

The ESP and geometry optimization of bidentate molecules were conducted on the Gaussian 09 program using B3LYP as the exchange-correlation function and 6-31G* basis sets with default spin mode at the gas phase.

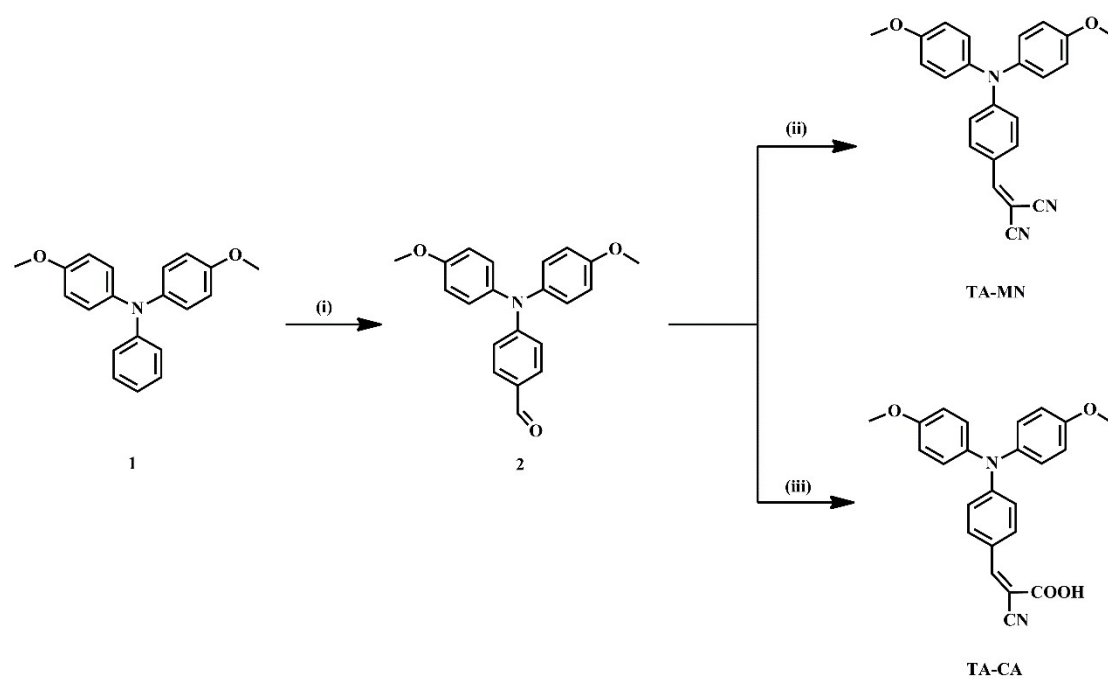
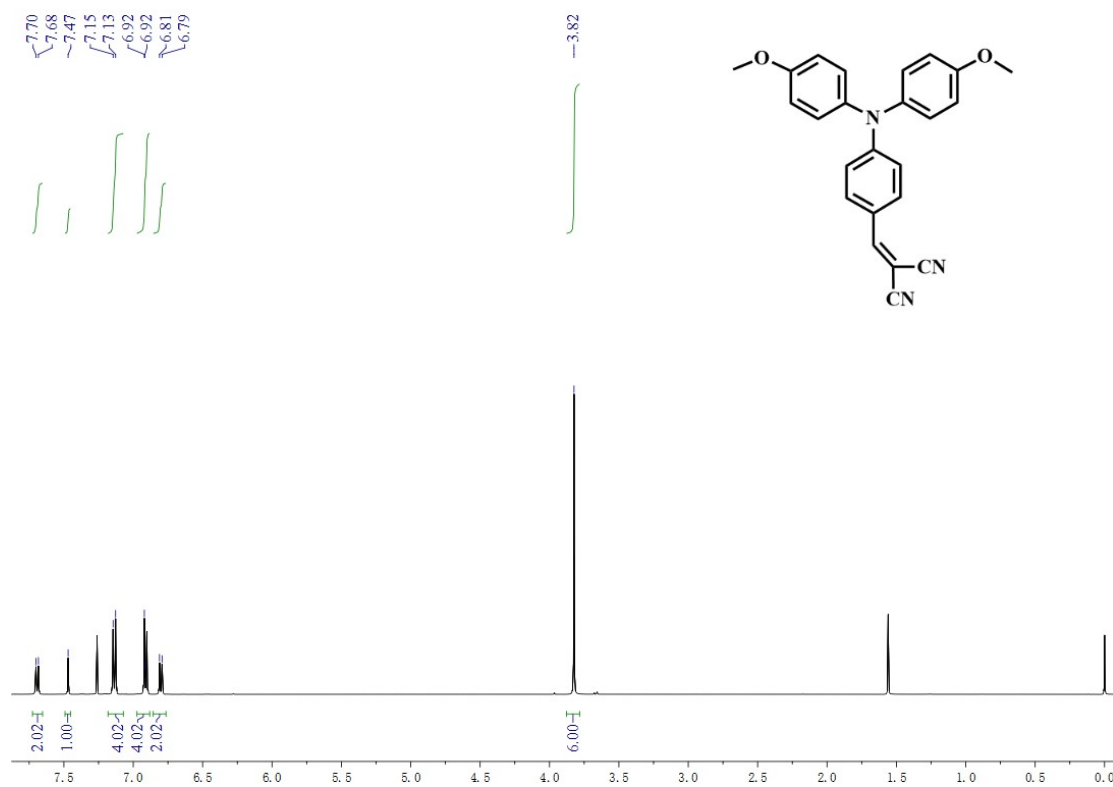


Fig. S1 Synthetic route to TA-MN and TA-CA. Reagents and conditions: i) POCl₃, DMF, stir at 90 °C for 3 h; ii) malononitrile, NaOAc, DMF, stir at RT for 3 h; iii) 2-cyanoacetic acid, NaOAc, DMF, stir at 60 °C for 6 h.

2.1 · ¹H-NMR



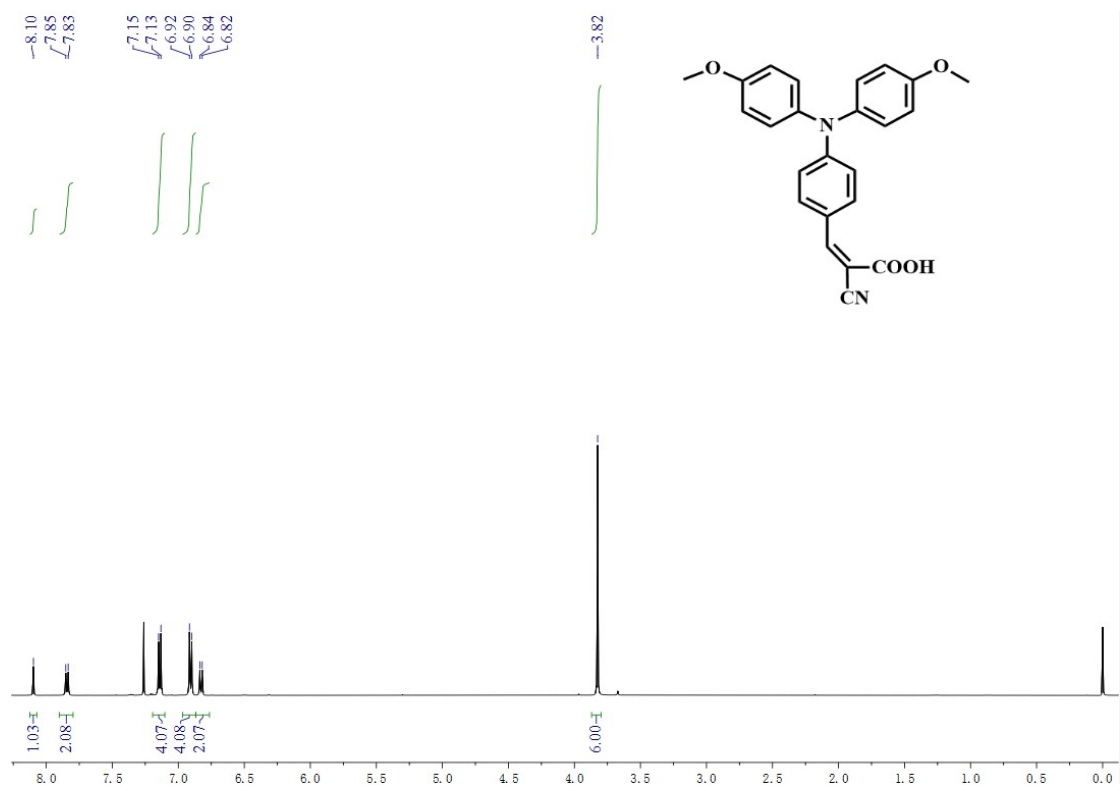


Fig. S3 $^1\text{H-NMR}$ of TA-CA.

2.2、 $^{13}\text{C-NMR}$

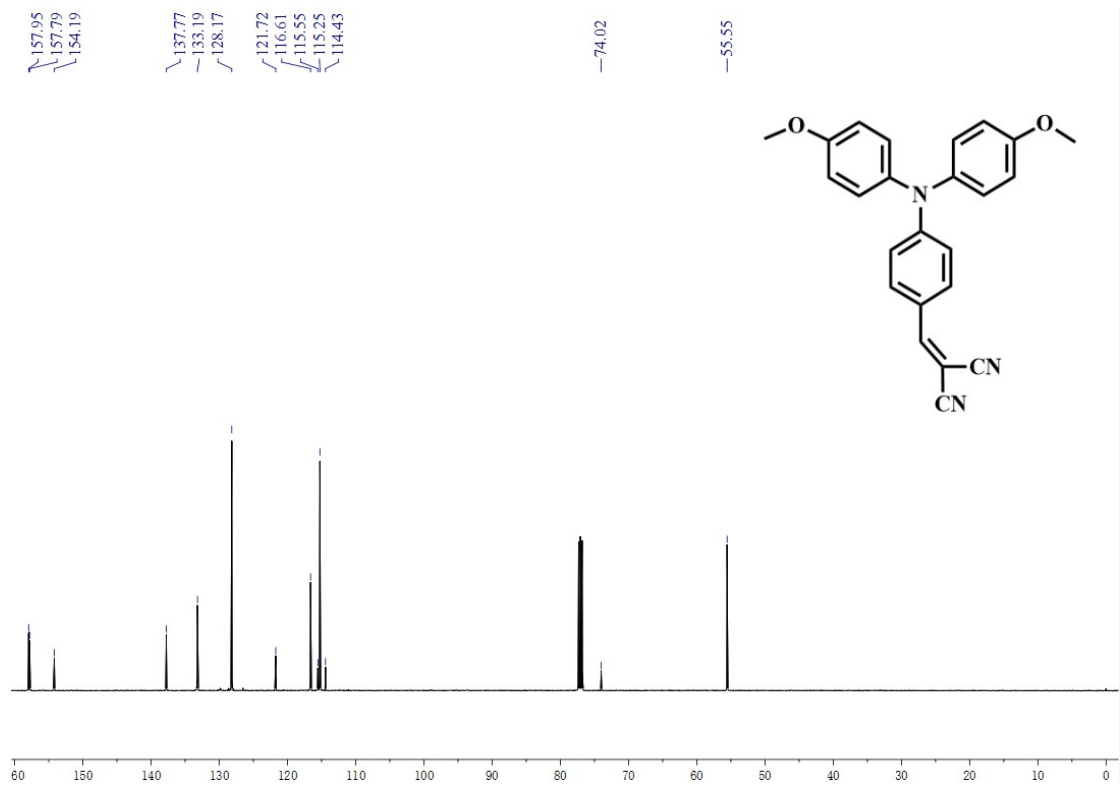


Fig. S4 $^{13}\text{C-NMR}$ of TA-MN.

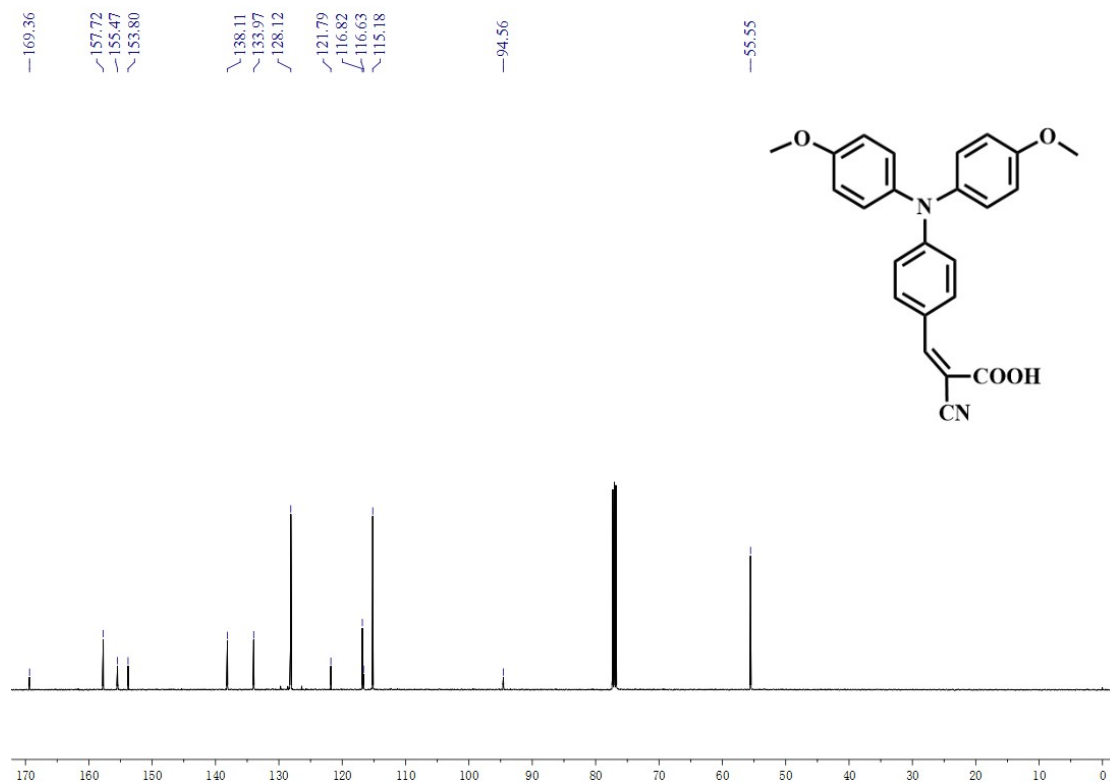


Fig. S5 ¹³C-NMR of TA-CA.

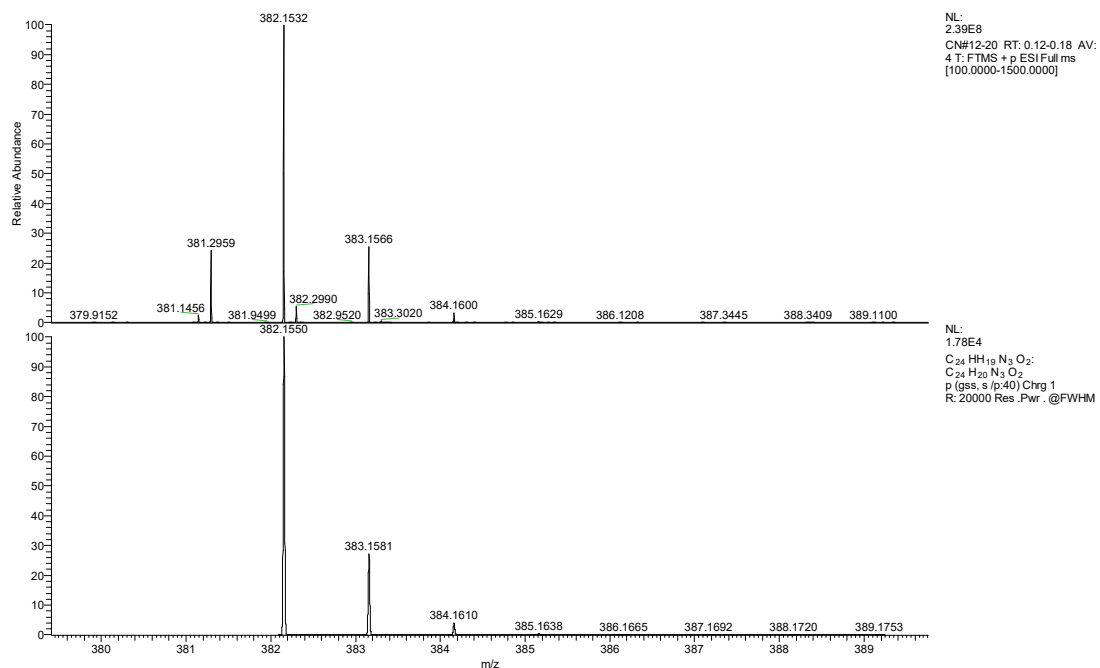


Fig. S6 UPLC-TOF MS spectrum of TA-MN.

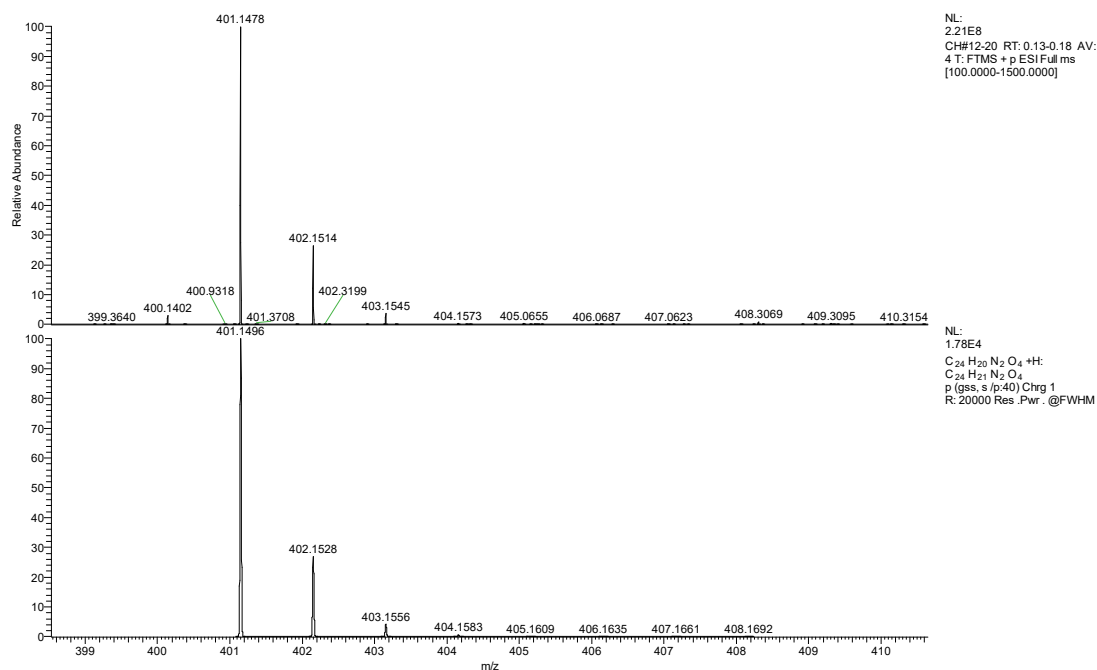


Fig. S7 UPLC-TOF MS spectrum of TA-CA.

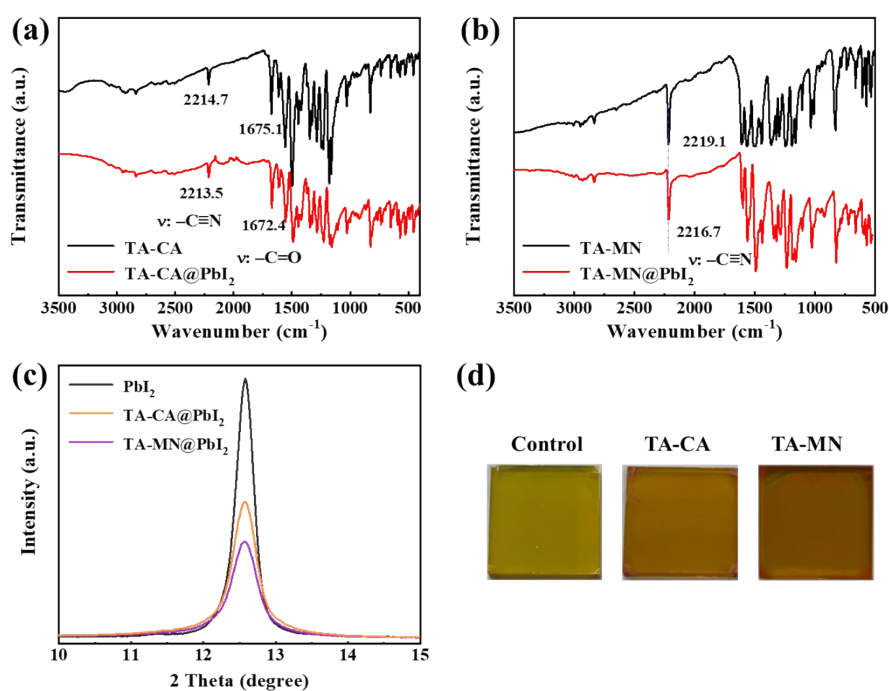


Fig. S8 (a-b) FTIR spectra of bidentate molecules and bidentate molecules mixture with PbI_2 , respectively, (c) XRD patterns of PbI_2 films without or with bidentate molecules, and (d) photography images of the PbI_2 films without or with bidentate molecules.

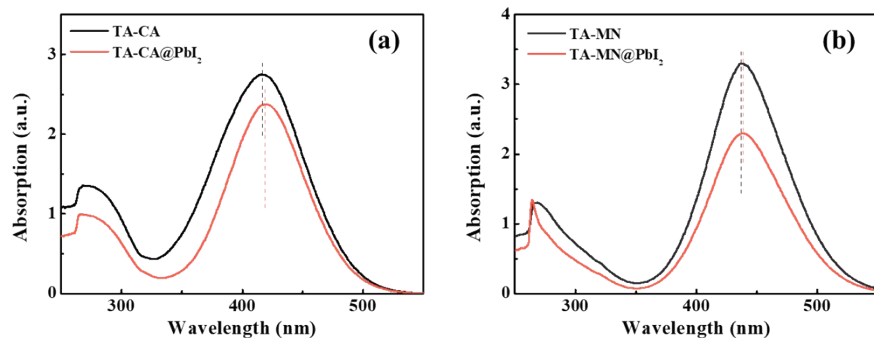


Fig. S9 UV-vis absorption spectra of (a) TA-CA, TA-CA@PbI₂, and (b)TA-MN-4, TA-MN@PbI₂ in the DMF solution.

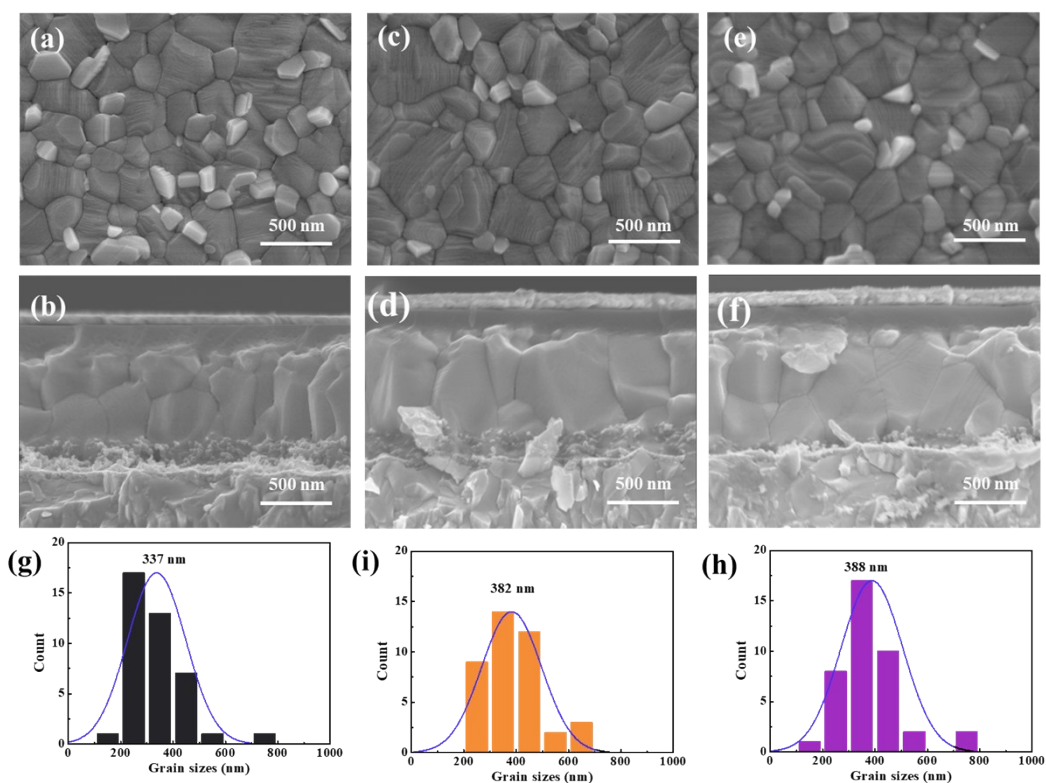


Fig. S10 Top-view and cross-sectional view SEM images of perovskite films without or with bidentate molecules passivation, and corresponding grain sizes distribution of perovskite films, (a,b,g) Control, (c,d,i) TA-CA, and (e,f,h) TA-MN.

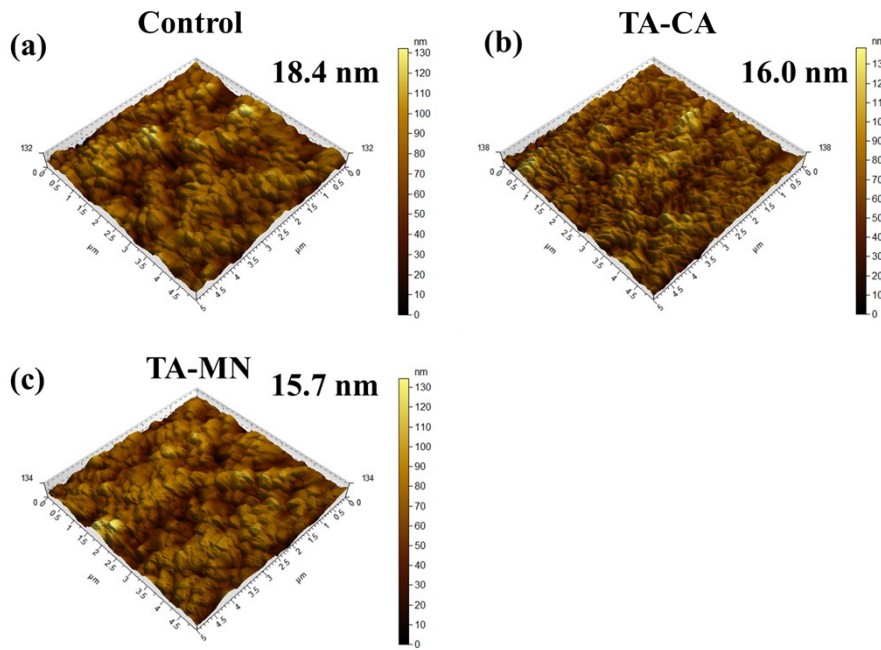


Fig. S11 The AFM images of the perovskite without and with bidentate molecules passivation.

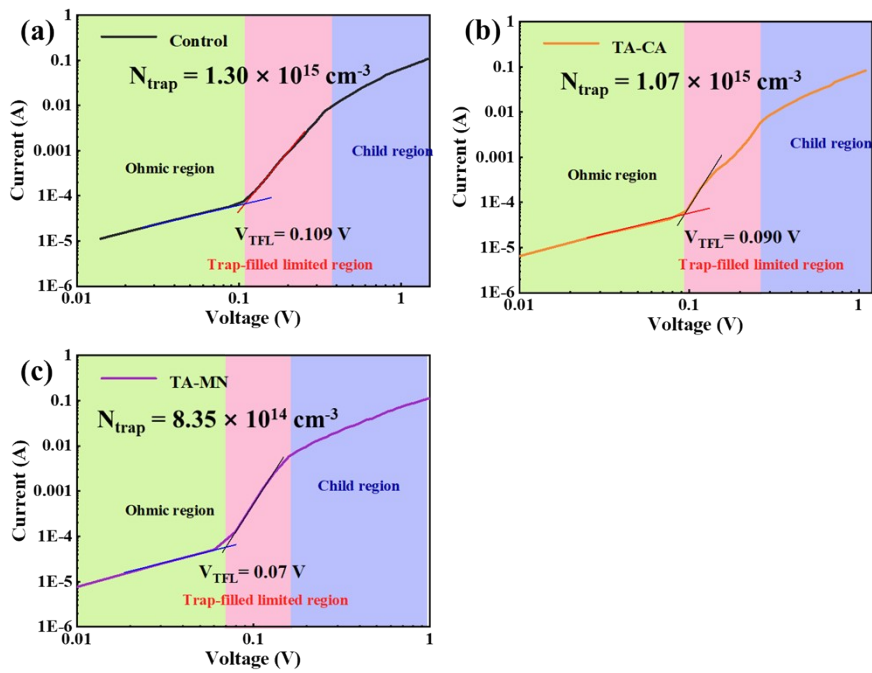


Fig. S12 Dark I - V curves of the hole-only device structure of FTO/ NiO_x /perovskite/spiro-OMeTAD/Au, (a) control, (b) TA-CA, and (c) TA-MN.

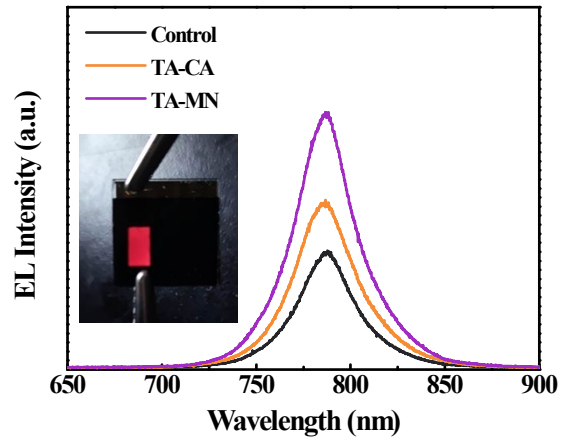


Fig. S13 The electroluminescence spectra (EL) of the devices with or without different bidentate passivators under 1.5 V bias in the dark operating.

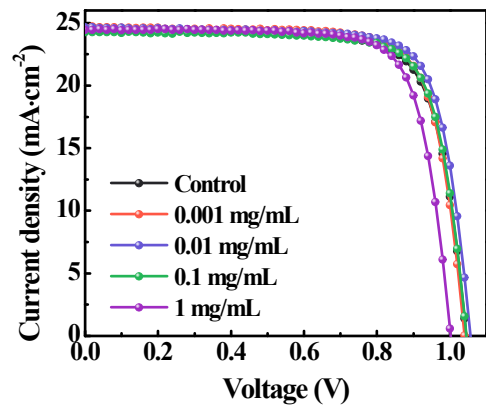


Fig. S14 $J-V$ curves of PSCs passivated by TA-CA with different concentrations.

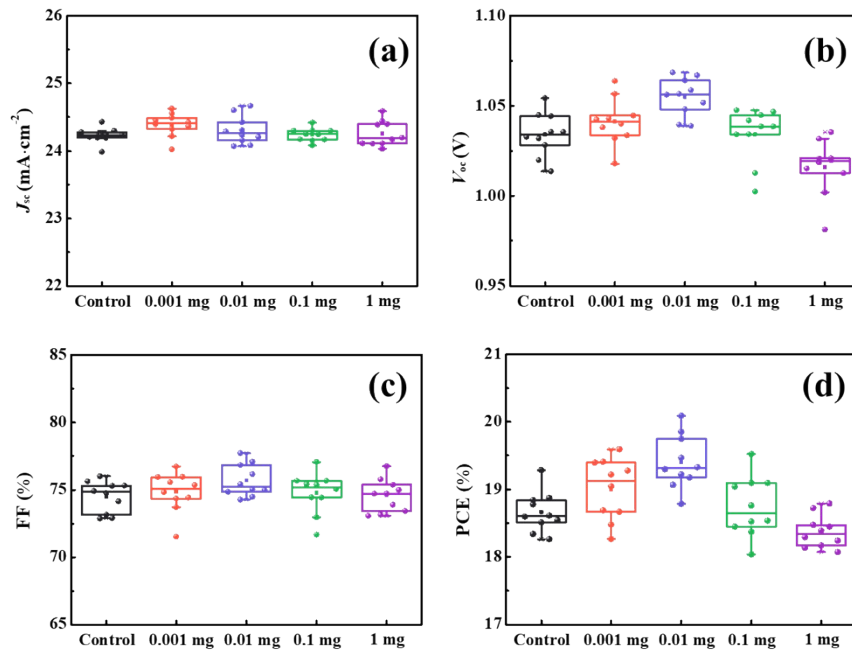


Fig. S15 Statistical distribution of photovoltaic parameters of (a) J_{SC} , (b) V_{OC} , (c) FF, and (d) PCE, obtained by J - V measurements of PSCs passivated by TA-CA with different concentrations.

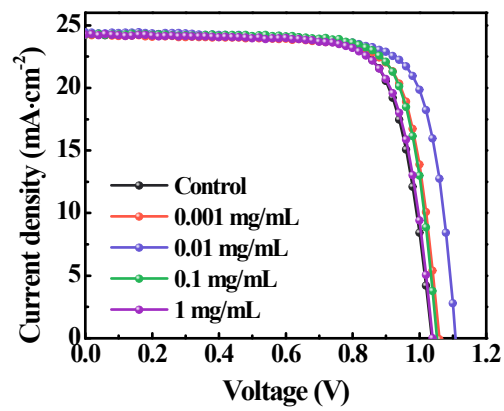


Fig. S16 J - V curves of PSCs passivated by TA-MN with different concentrations.

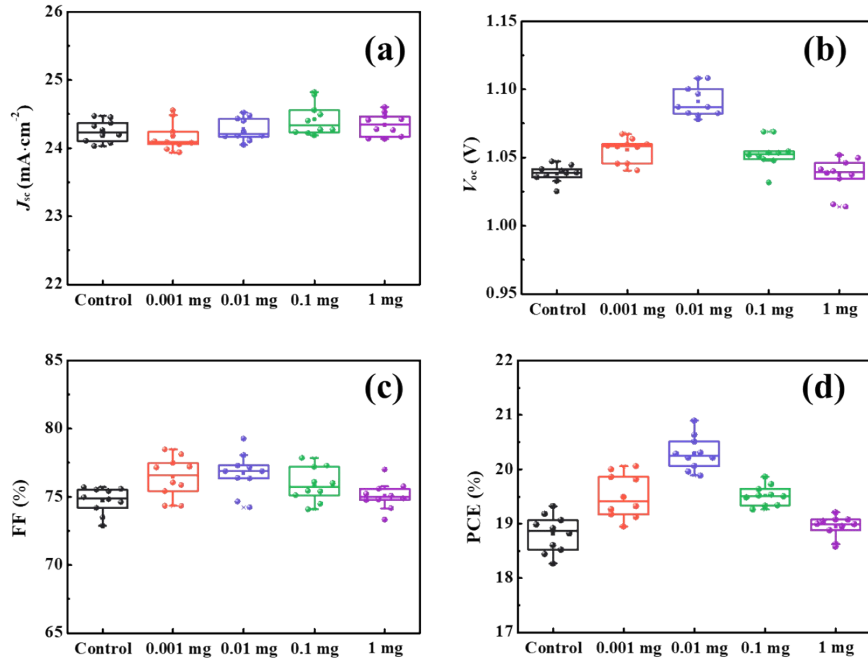


Fig. S17 Statistical distribution of photovoltaic parameters of (a) J_{sc} , (b) V_{oc} , (c) FF, and (d) PCE, obtained by J - V measurements of PSCs passivated by TA-MN with different concentrations.

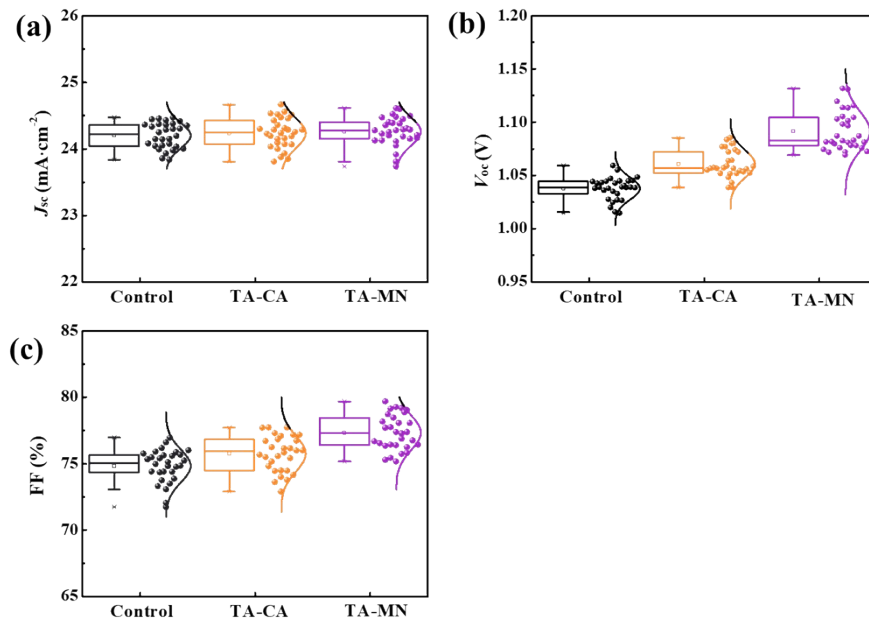


Fig. S18 Statistical distribution of photovoltaic parameters of (a) J_{sc} , (b) V_{oc} , and (c) FF obtained by J - V measurements of PSCs without and with bidentate molecules passivation.

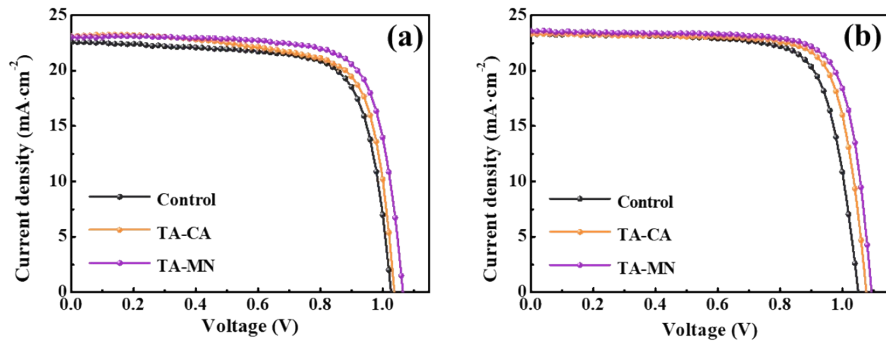


Fig. S19 J - V curves of the PSCs based on (a) MAPbI_3 , and (b) FAMA-based perovskite films without or with different bidentate passivators.

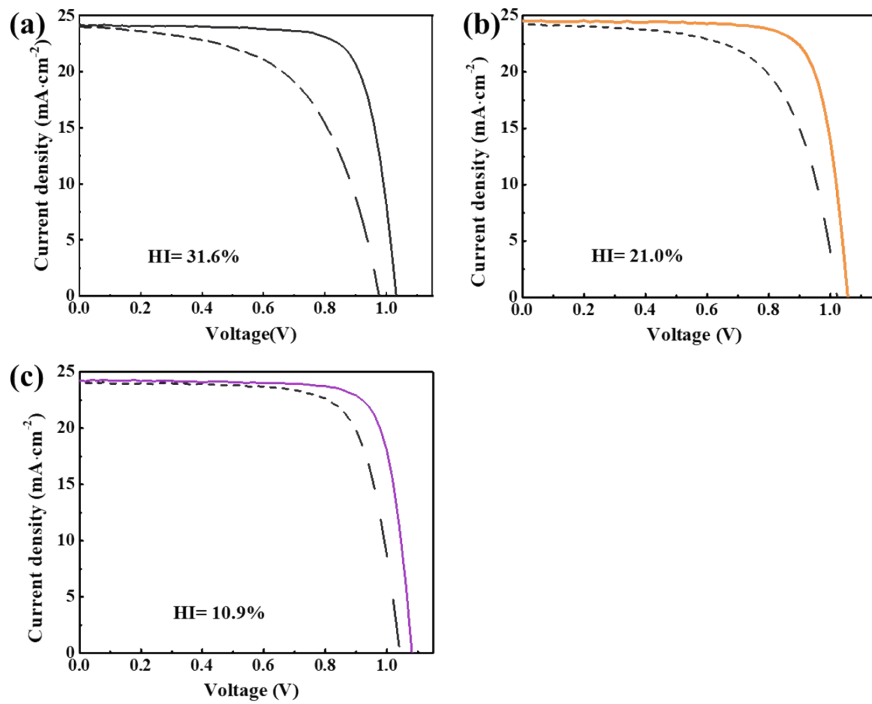


Fig. S20 J - V curves of the PSCs (a) without and with (b) TA-CA, (c) TA-MN at the reverse and forward scans.

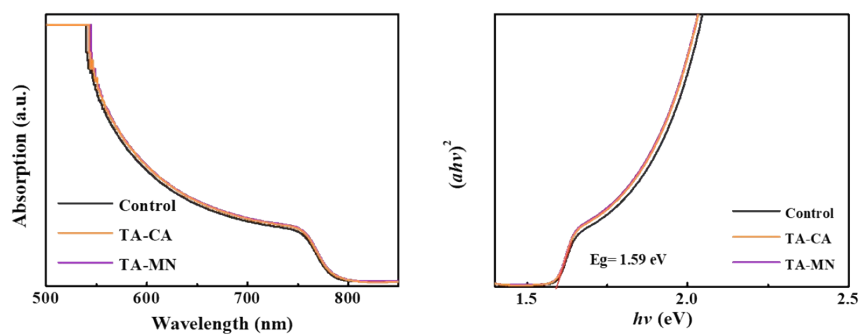


Fig. S21 The UV-vis absorption spectra and corresponding Tauc plots of perovskite films without and with bidentate molecules passivation.

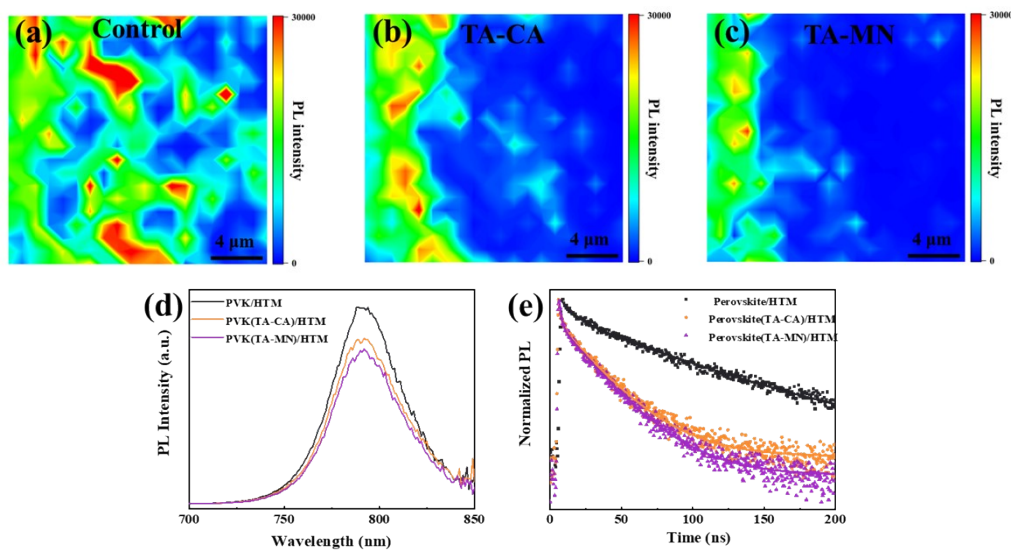


Fig. S22 (a-c) Confocal PL intensity mapping images, (d) the steady-state photoluminescence (PL) spectra, and (e) time-resolved photoluminescence of perovskite films without and with bidentate molecules passivation based on the structure of glass/perovskite/HTM.

Table S1 Crystallographic parameters of TA-CA and TA-MN.

| | TA-MN | TA-CA |
|------------------------------------|---|---|
| <i>Empirical formula</i> | C ₂₄ H ₁₉ N ₃ O ₂ | C ₂₄ H ₂₀ N ₂ O ₄ |
| <i>Formula weight</i> | 381.42 | 400.42 |
| <i>Crystal color</i> | orange | clear light red |
| <i>Crystal system</i> | triclinic | monoclinic |
| <i>a, Å</i> | 9.2334(5) | 12.767(8) |
| <i>b, Å</i> | 10.4165(6) | 10.420(7) |
| <i>c, Å</i> | 11.8908(7) | 15.834(11) |
| <i>α, deg</i> | 91.324(2) | 90 |
| <i>β, deg</i> | 108.779(2) | 99.035(18) |
| <i>γ, deg</i> | 108.854(2) | 90 |
| <i>V, Å³</i> | 1014.31(10) | 2080(2) |
| <i>ρ calc, g/cm³</i> | 1.249 | 1.278 |
| <i>Space group</i> | <i>P</i> -1 | <i>P</i> 1 2 ₁ / <i>n</i> 1 |
| <i>Z value</i> | 2 | 4 |
| <i>Temperature, K</i> | 200 (2) | 296.15 |
| <i>no. of reflections measured</i> | 3210 | 2877 |
| <i>no. of variables</i> | 264 | 840 |
| <i>Residuals: R; wR2</i> | 0.0550, 0.1651 | 0.0934, 0.1910 |

Table S2 Fitted data for TRPL decay based on the structure of glass/perovskite without and with bidentate molecules passivation.

| Sample | A ₁ (%) | τ ₁ (ns) | A ₂ (%) | τ ₂ (ns) | τ _{ave} (ns) ^[a] |
|---------|--------------------|---------------------|--------------------|---------------------|--------------------------------------|
| Control | 4.48 | 86.98 | 95.52 | 700.39 | 696.8 |
| TA-CA | 1.71 | 61.66 | 98.29 | 933.14 | 932.0 |
| TA-MN | 1.21 | 42.75 | 98.79 | 1172.59 | 1172.1 |

$$[a] \tau_{ave} = \frac{\sum A_i \tau_i^2}{\sum A_i \tau_i}$$

Table S3 EIS parameters of PSCs without and with different bidentate molecules passivation under the dark condition at bias.

| Device | R_s (Ω) | R_{rec} (Ω) |
|---------|--------------------|------------------------|
| Control | 9.81 | 2918 |
| TA-CA | 7.30 | 4068 |
| TA-MN | 7.56 | 5722 |

Table S4 Photovoltaic parameters for the champion PSCs with the passivation of TA-CA at different concentrations.

| TA-CA | J_{SC} ($\text{mA}\cdot\text{cm}^{-2}$) | V_{OC} (V) | FF (%) | PCE (%) |
|-------------|---|--------------|--------|---------|
| 0 | 24.30 | 1.044 | 76.00 | 19.28 |
| 0.001 mg/mL | 24.56 | 1.040 | 76.72 | 19.59 |
| 0.01 mg/mL | 24.66 | 1.057 | 77.09 | 20.09 |
| 0.1 mg/mL | 24.24 | 1.045 | 77.06 | 19.52 |
| 1 mg/mL | 24.44 | 1.002 | 76.75 | 18.79 |

Table S5 Photovoltaic parameters for the champion PSCs with TA-MN passivation at different concentrations.

| TA-MN | J_{SC} ($\text{mA}\cdot\text{cm}^{-2}$) | V_{OC} (V) | FF (%) | PCE (%) |
|-------------|---|--------------|--------|---------|
| 0 | 24.33 | 1.038 | 75.67 | 19.20 |
| 0.001 mg/mL | 24.24 | 1.060 | 77.15 | 19.82 |
| 0.01 mg/mL | 24.43 | 1.108 | 77.16 | 20.89 |
| 0.1 mg/mL | 24.22 | 1.054 | 77.84 | 19.86 |
| 1 mg/mL | 24.26 | 1.040 | 75.58 | 19.07 |

Table S6 Photovoltaic parameters of PSCs based on MAPbI₃ and FAMA-based perovskite films without or with different bidentate passivators.

| Perovskite | Device | J_{SC} ($\text{mA}\cdot\text{cm}^{-2}$) | V_{OC} (V) | FF (%) | PCE (%) |
|--------------------|---------|---|--------------|--------|---------|
| MAPbI ₃ | Control | 22.60 | 1.027 | 73.61 | 17.08 |
| | TA-CA | 23.09 | 1.038 | 73.55 | 17.63 |
| | TA-MN | 23.03 | 1.061 | 75.68 | 18.56 |
| FAMA-based | Control | 23.31 | 1.051 | 75.38 | 18.47 |
| | TA-CA | 23.32 | 1.077 | 77.77 | 19.54 |
| | TA-MN | 23.58 | 1.094 | 77.94 | 20.11 |

Table S7 Photovoltaic parameters of champion PSCs of the control device and with the passivation of TA-CA and TA-MN at the reverse and forward scans.

| Device | Scan directions | J_{SC} (mA·cm ⁻²) | V_{OC} (V) | FF (%) | PCE (%) | HI (%) ^[b] |
|---------|-----------------|---------------------------------|--------------|--------|---------|-----------------------|
| Control | Forward | 24.01 | 0.977 | 56.89 | 13.34 | 31.6 |
| | Reverse | 24.21 | 1.033 | 76.38 | 19.10 | |
| TA-CA | Forward | 24.22 | 1.022 | 64.26 | 15.90 | 21.0 |
| | Reverse | 24.51 | 1.057 | 77.70 | 20.12 | |
| TA-MN | Forward | 24.00 | 1.042 | 73.75 | 18.46 | 10.9 |
| | Reverse | 24.25 | 1.081 | 79.03 | 20.72 | |

$$[b] \quad HI = \frac{PCE_{Reverse} - PCE_{Forward}}{PCE_{Reverse}}$$

Table S8 Fitted data for TRPL decay based on the structure of glass/perovskite/HTM without and with bidentate molecules.

| Sample | A ₁ (%) | τ_1 (ns) | A ₂ (%) | τ_2 (ns) | τ_{ave} (ns) |
|---------|--------------------|---------------|--------------------|---------------|-------------------|
| Control | 3.70 | 11.49 | 96.30 | 89.32 | 88.94 |
| TA-CA | 3.86 | 1.81 | 96.14 | 30.47 | 30.40 |
| TA-MN | 4.66 | 1.73 | 95.34 | 30.25 | 29.98 |